Multi-pulse oscillation and instabilities in microchip self-Q-switched transverse-mode laser

Jun Dong[1,2*], Ken-ichi Ueda[2], Peizhi Yang[3]

[1]*Department of Electronics Engineering, School of Information Science and Technology, Xiamen University, Xiamen 361005, China*
[2] *Institute for Laser Science, University of Electro-Communications, 1-5-1 Chofugaoka, Chofu, Tokyo 182-8585, Japan*
[3] *Key Laboratory of Advanced Technique & Preparation for Renewable Energy Materials, Ministry of Education, Yunnan Normal University, Kunming 650092, China*
* jdong@xmu.edu.cn

Abstract: Multi-transverse-mode competition, coupling induced instabilities and multi-pulse or satellite pulse oscillations were investigated experimentally and theoretically in laser-diode-pumped Cr,Nd:YAG self-Q-switched microchip lasers under large pump beam diameter. The different transverse modes have great effects on the laser pulse temporal characteristics such as pulse profile, pulse width, instability of peak power and repetition rate jitter. Multi-transverse-mode, multi-pulse oscillation and periodical pulsation were observed by varying the pump beam diameter. The effect of transverse modes on the instability and multi-pulse oscillation were studied by modified coupled rate equations by taking into account the transverse-mode competition of inversion population under different pump conditions. The numerically simulated results are in good agreement with the experimental results. These results show that the multi-pulse oscillation and instability in the pulse train were attributed to different transverse mode coupling and competition. The peak power instabilities and pulse repetition rate jitter of the laser pulses due to transverse mode coupling were also investigated.

©2009 Optical Society of America

OCIS codes: (190.3100) Instabilities and chaos; (140.3480) Lasers, diode-pumped; (140.3540) Lasers, Q-switched.

References and links

1. J. J. Zayhowski, "Passively Q-switched Nd:YAG microchip lasers and applications," J. Alloy. Comp. **303–304**(1-2), 393–400 (2000).
2. G. J. Spuhler, R. Paschotta, M. P. Kullberg, M. Graf, M. Moser, E. Mix, G. Huber, C. Harder, and U. Keller, "A passively Q-switched Yb:YAG microchip laser," Appl. Phys. B: Lasers Opt. **72**, 285–287 (2001).
3. J. Dong, P. Deng, Y. Liu, Y. Zhang, J. Xu, W. Chen, and X. Xie, "Passively Q-Switched Yb:YAG Laser with Cr(4+):YAG as the Saturable Absorber," Appl. Opt. **40**(24), 4303–4307 (2001).
4. J. J. Zayhowski, and C. Dill III, "Diode-pumped passively Q-switched picosecond microchip lasers," Opt. Lett. **19**(18), 1427–1429 (1994).
5. J. Dong, A. Shirakawa, and K. Ueda, "Sub-nanosecond passively Q-switched Yb:YAG/Cr⁴⁺:YAG sandwiched microchip laser," Appl. Phys. B: Lasers Opt. **85**(4), 513–518 (2006).
6. J. Dong, and K. Ueda, "Longitudinal-mode competition induced instabilities of Cr⁴⁺,Nd³⁺:Y₃Al₅O₁₂ self-Q-switched two-mode laser," Appl. Phys. Lett. **87**(15), 151102 (2005).
7. M. Wei, C. Cheng, and S. Wu, "Instability and satellite pulse of passively Q-switching Nd:LuVO₄ laser with Cr⁴⁺:YAG saturable absorber," Opt. Commun. **281**(13), 3527–3531 (2008).
8. J. Dong, A. Shirakawa, and K. Ueda, "Switchable pulses generation in passively Q-switched multilongitudinal-mode microchip laser," Laser Phys. Lett. **4**(2), 109–116 (2007).
9. S. Longhi, "Theory of transverse modes in end-pumped microchip lasers," J. Opt. Soc. Am. B **11**(6), 1098–1107 (1994).
10. J. J. Degnan, "Optimization of passively Q-switched lasers," IEEE J. Quantum Electron. **31**(11), 1890–1901 (1995).
11. J. Dong, and K. Ueda, "Observation of repetitively nanosecond pulse-width transverse patterns in microchip self-Q-switched laser," Phys. Rev. A **73**(5), 053824 (2006).

12. S. P. Hegarty, G. Huyet, P. Porta, J. G. McInerney, K. D. Choquette, K. M. Geib, and H. Q. Hou, "Transverse-mode structure and pattern formation in oxide-confined vertical-cavity semiconductor lasers," J. Opt. Soc. Am. B **16**(11), 2060–2071 (1999).
13. K. Otsuka, P. Mandel, and E. A. Viktorov, "Breakup of cw multimode oscillations and low-frequency instability in a microchip solid-state laser by high-density pumping," Phys. Rev. A **56**(4), 3226–3232 (1997).
14. Y. F. Chen, and Y. P. Lan, "Spontaneous transverse pattern formation in a microchip laser excited by a doughnut pump profile," Appl. Phys. B **75**(4-5), 453–456 (2002).
15. Y. F. Chen, and Y. P. Lan, "Observation of transverse patterns in an isotropic microchip laser," Phys. Rev. A **67**(4), 043814 (2003).
16. G. K. Harkness, and W. J. Firth, "Transverse modes of microchip solid state lasers," J. Mod. Opt. **39**(10), 2023–2037 (1992).
17. A. A. Ishaaya, N. Davidson, and A. A. Friesem, "Very high-order pure Laguerre-Gaussian mode selection in a passive Q-switched Nd:YAG laser," Opt. Express **13**(13), 4952–4962 (2005).
18. M. D. Wei, C. H. Chen, and K. C. Tu, "Spatial and temporal instability in a passively Q-switched Nd:YAG laser with a Cr^{4+}:YAG saturable absorber," Opt. Express **12**(17), 3972–3980 (2004).
19. S. Longhi, G. Cerullo, S. Taccheo, V. Magni, and P. Laporta, "Experimental observation of transverse effects in microchip solid-state laser," Appl. Phys. Lett. **65**(24), 3042–3044 (1994).
20. S. P. Ng, D. Y. Tang, L. J. Qian, and L. J. Qin, "Satellite pulse generation in diode-pumped passively Q-switched Nd:$GdVO_4$ lasers," IEEE J. Quantum Electron. **42**(7), 625–632 (2006).
21. T. Taira, J. Saikawa, T. Kobayashi, and R. L. Byer, "Diode-pumped tunable Yb:YAG miniature lasers at room temperature: modeling and experiment," IEEE J. Sel. Top. Quantum Electron. **3**(1), 100–104 (1997).
22. C. L. Tang, H. Statz, and G. Demars, "Spectral output and spiking behavior of solid-state lasers," J. Appl. Phys. **34**(8), 2289–2295 (1963).
23. K. Otsuka, M. Georgiou, and P. Mandel, "Intensity fluctuations in multimode lasers with spatial hole burning," Jpn. J. Appl. Phys. **31**(Part 2, No. 9A), L1250–L1252 (1992).
24. K. Otsuka, J. Y. Ko, T. Kubota, S. L. Hwong, T. S. Lim, J. L. Chern, B. A. Nguyen, and P. Mandel, "Instability in a laser-diode-pumped microchip Nd:YAG laser in a n-ary product scheme," Opt. Lett. **26**(14), 1060–1062 (2001).
25. J. Dong, "Numerical modeling of CW-pumped repetitively passively Q-switched Yb:YAG lasers with Cr:YAG as saturable absorber," Opt. Commun. **226**(1-6), 337–344 (2003).
26. R. Oron, L. Shimshi, S. Blit, N. Davidson, A. A. Friesem, and E. Hasman, "Laser operation with two orthogonally polarized transverse modes," Appl. Opt. **41**(18), 3634–3637 (2002).
27. X. Zhang, S. Zhao, Q. Wang, Q. Zhang, L. Sun, and S. Zhang, "Optimization of Cr^{4+}-doped saturable-absorber Q-switched lasers," IEEE J. Quantum Electron. **33**(12), 2286–2294 (1997).
28. Y. Shimony, Z. Burshtein, and Y. Kalisky, "Cr^{4+}:YAG as passive Q-switch and Brewster plate in a Nd:YAG laser," IEEE J. Quantum Electron. **31**(10), 1738–1741 (1995).
29. Z. Burshtein, P. Blau, Y. Kalisky, Y. Shimony, and M. R. Kikta, "Excited-state absorption studies of Cr^{4+} ions in several garnet host crystals," IEEE J. Quantum Electron. **34**(2), 292–299 (1998).
30. H. Eilers, K. R. Hoffman, W. M. Dennis, S. M. Jacobsen, and W. M. Yen, "Saturation of 1.064 μm absorption in Cr,Ca:$Y_3Al_5O_{12}$ crystals," Appl. Phys. Lett. **61**(25), 2958–2960 (1992).
31. G. Xiao, J. H. Lim, S. Yang, E. V. Stryland, M. Bass, and L. Weichman, "Z-scan measurement of the ground and excited state absorption cross section of Cr^{4+} in yttrium aluminum garnet," IEEE J. Quantum Electron. **35**(7), 1086–1091 (1999).
32. J. Dong, J. Lu, and K. Ueda, "Experiments and numerical simulation of a diode-laser-pumped Cr,Nd:YAG self-Q-switched laser," J. Opt. Soc. Am. B **21**(12), 2130–2136 (2004).
33. J. Dong, P. Deng, Y. Lu, Y. Zhang, Y. Liu, J. Xu, and W. Chen, "Laser-diode-pumped Cr(4)+, Nd(3)+:YAG with self-Q-switched laser output of 1.4 W," Opt. Lett. **25**(15), 1101–1103 (2000).
34. B. Lipavsky, Y. Kalisky, Z. Burshtein, Y. Shimony, and S. Rotman, "Some optical properties of Cr^{4+} - doped crystals," Opt. Mater. **13**(1), 117–127 (1999).
35. W. Koechner, *Solid State Laser Engineering* (Springer-Verlag, Berlin, 1999), Chap. 2.

1. Introduction

Stable, high beam quality, passively Q-switched lasers with high peak power are good laser sources for light detecting and ranging, pollution monitoring, materials processing, microsurgery, and so on [1]. Passively Q-switched solid-state lasers are usually operated by using Nd^{3+} or Yb^{3+} doped materials as gain media and Cr^{4+}:YAG crystal or semiconductor saturable absorber mirror (SESAM) as saturable absorber [1–3]. Pulses with sub-nanosecond durations and several tens of kilowatt peak power have been achieved [4,5]. However, passively Q-switched pulses under multi-mode oscillation usually exhibit large jitter in peak power and in repetition rate that are undesirable for many applications [6–8]. Stable laser operation can be realized when the laser is working at single-frequency, TEM_{00} mode, which is usually operating at low pump power [6] with a spatially narrow pump width which improves the stability of the fundamental transverse mode [9]. However, there will be longitudinal-mode competition induced peak power instability and repetition rate jitter under

high pump power with spatial narrow pump width [6]. And according to the passively Q-switched laser theory [10], the output pulse energy of passively Q-switched lasers cannot be further increased at high pump power with spatially narrow pump width when the saturable absorber is fully saturated. The pulse energy and pulse width are determined mainly by: the initial transmission of the saturable absorber, intracavity loss and laser mode volume; they are independent on the pump power. Therefore, pulse energy scaling for passively Q-switched laser can be realized by increasing the laser mode volume which can be achieved by increasing the pump beam diameter at high pump power levels and at the same time keeping single-frequency laser oscillation. However, increase pump beam diameter on the gain medium will allow multi-transverse-mode oscillation [11], which will introduce instabilities on the laser pulse amplitude and repetition rate jitter. For laser-diode end-pumped microchip lasers, the planar symmetry of the flat-flat cavity is broken by the pump beam, and thermal effects and gain-guiding effects control the formation of the transverse modes. These transverse modes will have great effects on the laser pulse characteristics such as pulse profiles and output pulse trains, the pulse profiles will exhibit satellite-like pulses or multi-pulse oscillation and the output pulse trains will exhibit periodical oscillation or chaos [7].

Recently, transverse pattern formation has been observed in vertical cavity surface emitting semiconductor lasers with large transverse cross-section and short cavity length [12]. Single-longitudinal-mode oscillation was easily obtained in vertical cavity surface emitting semiconductor lasers owing to its very short cavity and by eliminating the influence of other degrees of freedom such as cavity configurations, pump beam distribution and so on [12]. Therefore, it was useful to study transverse patterns formed by coupling and competing of different transverse modes. However, the main difficulty for analysis is that transverse pattern formation is strongly sensitive to the homogeneity of the semiconductor wafers. Laser diode pumped microchip solid-state lasers have gained much attention for studying transverse pattern formation [13] because they are more robust, homogeneous and less sensitive to thermal effects than semiconductor wafer. Because laser-diode pumped microchip laser can be easily operated in single-longitudinal-mode oscillation, the dynamics of transverse mode oscillation for laser-diode pumped microchip lasers can be fully investigated. Experimental and theoretical investigations on transverse mode pattern formation of laser-diode pumped microchip solid-state lasers have been reported [9,14–16]. However, these microchip lasers were usually operated in continuous-wave mode and the transverse pattern formation was affected by the laser cavity. The applications (such as optical information processing, chemical or biological spectral analyzes and so on) of pattern formation require high peak power pulse lasers, which can be realized by passively Q-switched solid-state laser. High peak power passively Q-switched solid-state lasers are usually achieved by using high gain medium and Cr^{4+}:YAG as a saturable absorber [1]. Recently there are some reports on the laser instabilities of Cr^{4+}:YAG passively Q-switched Nd:YAG lasers induced by transverse mode competition [17,18]. However, the experimental results strongly depend on the cavity parameters, and transverse pattern formation in such lasers was also affected by cavity tuning. In this study the dynamics of transverse pattern formation due to the cavity variation and the pump power were not fully understood. The best way to understand such interesting phenomena is to separate the factors (the cavity configuration and the pump beam waist, and so on) that have effects on transverse pattern formation. Because self-Q-switched microchip lasers have simple, short, plane-parallel cavities, single-longitudinal-mode oscillation can be easily obtained by adopting a suitable pump power intensity, which makes it a very good choice to study the effect of transverse modes on the laser instabilities.

For plane-parallel microchip laser resonator, the output power can be scaled by increasing the pump beam area on the gain medium. Most of the pump beams from laser diode are usually in Gaussian distribution or top-hat profile. At the same pump power, the pump power intensity on the gain medium will decrease with increase of the pump beam area. The pump power distribution inside the gain medium will become more uniform compared to the high pump intensity at smaller pump beam diameter, which will give rise to different transverse-mode oscillation. The mode width and the pump power threshold have approximately the

same values for all transverse modes under a broad pump beam [9,16]. Experimental observation of the transverse mode effect in continuous-wave microchip solid-state lasers has been reported [19]. The effect of the pump beam waist on transverse-mode formation was reported, and was in good agreement with the theoretical prediction with the mechanism that controls the transverse modes by balancing diffraction and focusing effects induced by the pump beam [9]. Recently, complex transverse pattern formation was observed in laser-diode pumped Cr,Nd:YAG microchip lasers, although there are some reports on the effect of the transverse mode on the pulse characteristics and periodical pulse trains [7,11,18,20], however, to our best knowledge, the mechanics of the transverse mode on the laser pulse characteristics of passively Q-switched microchip lasers were not clearly stated. Therefore, in this paper, the effect of the transverse modes of Cr,Nd:YAG self-Q-switched microchip laser on laser pulse generation and periodical pulse trains is investigated. The instabilities induced by the transverse mode competition and coupling were also observed by measuring the temporal laser pulse characteristics (pulse repetition rate and pulse profiles) at different pumping conditions. The modified rate equations with multi-transverse-mode coupling were proposed and numerical simulation of the effect of multi-transverse-mode on the laser pulse characteristics and periodical pulse trains are in good agreement with experimental results, these results show that the multiple pulse generation and periodical pulse train are related to the transverse mode competition and coupling.
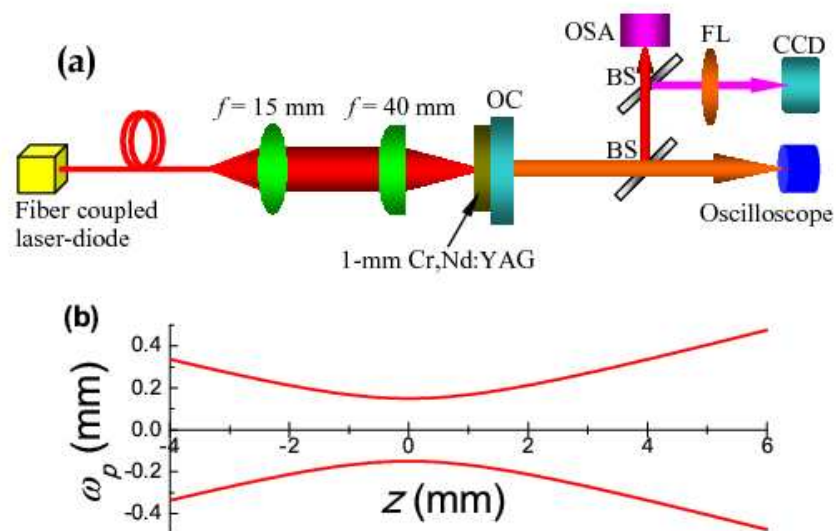
2. Experiments

Fig. 1. (a) Schematic diagram of experimental setup used to observe instabilities and multiple-pulse oscillation in a laser-diode pumped microchip Cr,Nd:YAG self-Q-switched laser, BS, beam splitter; FL, focal lens; OC, output coupler; (b) Variation of the pump beam waist with position of the Cr,Nd:YAG sample.

Figure 1(a) shows the schematic diagram of an end-pumped microchip Cr,Nd:YAG self-Q-switched laser [11]. The gain medium is a plane-parallel, 1-mm-thick Cr,Nd:YAG crystal co-doped with 1 at.% Nd and 0.01 at.% Cr. One surface of the crystal is coated for high transmission at 808 nm and total reflection at 1064 nm. The other surface is coated for antireflection at 1064 nm and total reflection at 808 nm to increase the absorption of the pump power. A plane-parallel output coupler with 5% transmission at 1064 nm was mechanically attached to the Cr,Nd:YAG crystal. A 3-W fiber-coupled 807 nm laser-diode with a fiber core diameter of 400 μm and numerical aperture of 0.4 was used as the pump source. The coupling

optics (two lenses with focal length of $f = 15$ mm and $f = 40$ mm, respectively) were used to focus the pump beam into the crystal rear surface and to produce a pump light spot size in the crystal of about 300 μm in diameter. When the pump beam on the gain medium is assumed to be Gaussian beam, using a beam quality factor, M^2, the radius of the pump beam along the direction of the light propagation can be expressed as [21]

$$\omega_p^2(z) = \omega_0^2 \left[1 + \frac{\left(M^2\right)^2 \lambda_p^2 \left(z - z_0\right)^2}{n^2 \pi^2 \omega_0^4} \right] \qquad (1)$$

where z is the coordinate along the axis of the laser, $\omega_p(z)$ is the radii of the pump beam at z, ω_0 is the radius of the pump beam at $z = z_0$, λ_p is the wavelength of the pump and the laser, n is the refractive index of the gain media. For the laser experimental setup shown in Fig. 1(a), the pump beam radius at different position, as shown in Fig. 1(b), can be estimated according to the Eq. (1). The Rayleigh length of the pump beam with our current coupling optics was 2 mm, which was longer than the thickness of Cr,Nd:YAG crystal. The effect of the pump beam diameter on the Cr,Nd:YAG self-Q-switched laser performance was done by moving the Cr,Nd:YAG samples along the pump direction. The laser was operated at room temperature. The Q-switched pulses were recorded by using a fast InGaAs detector of less than 1-ns rise time, and a 500-MHz Tektronix TDS 3052B-digitizing oscilloscope. The laser spectrum was analyzed by using an optical spectrum analyzer. The laser output beam profile was monitored using a CCD camera both in the near field and the far field of the output coupler.
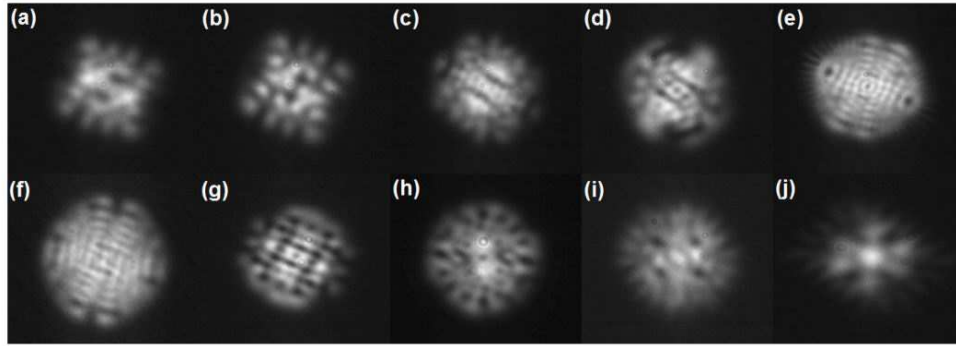
3. Results and discussion

Fig. 2. Transverse patterns of Cr,Nd:YAG self-Q-switched laser at different Cr,Nd:YAG sample positions, z, along the pump beam direction, (a) −3.5 mm, (b) −3 mm, (c) −2 mm, (d) −0.5 mm, (e) 0, (f) 1 mm, (g) 2 mm, (h) 3 mm, (i) 4 mm, (j) 5 mm.

To obtain stable transverse patterns in this self-Q-switched laser, the Cr,Nd:YAG self-Q-switched laser was operated at 1.5 times above the pump power threshold when the rear surface of the Cr,Nd:YAG is just on the focus position of the pump beam. By moving the Cr,Nd:YAG crystal along the pump beam direction, different sets of the transverse patterns were observed. Figure 2 shows different sets of the transverse patterns observed by moving the Cr,Nd:YAG crystal along the pump direction, which have been reported in detail previously [11]. All observed transverse patterns have point symmetry, are very stable, reproducible with no variation in the structure over time scales of hours. Transition between two different sets of transverse patterns was found to be sudden and abruptly with slowly and gradually moving Cr,Nd:YAG crystal along the pump beam direction. Furthermore, all observed transverse patterns were preserved in free-space propagation. Although all observed transverse patterns have point symmetry and some of them are nearly circular (z > −2 mm), they are different from high-order Laguerre-Gaussian modes. It is well known that only Hermite-Gaussian modes remain Hermite-Gaussian field patterns as they propagate.

Therefore, the formation of observed transverse patterns by varying the sample positions along the pump beam direction can be explained as a combination of different sets of Hermite-Gaussian modes. The $z = 0$ coordinate corresponds to a minimum measured pump beam waist of 150 μm just on the incident surface of the Cr,Nd:YAG crystal. Negative displacement of the Cr,Nd:YAG sample from $z = 0$ indicates that the sample is close the focus lens, positive displacement indicates the sample is far away from the focus lens, as shown in Fig. 1. The pump power intensity on the rear surface of the gain medium varies with the propagation position of the pump beam can be estimated according to the expression as follows,

$$I(z,r) = \frac{P_{in}}{\pi \omega_p^2(z)} \exp\left(-\frac{2r^2}{\omega_p^2(z)} \right) \qquad (2)$$

where z is the propagation direction of the pump beam, r is the radius of the pump beam at z position, P_{in} is the incident pump power on the rear surface of the gain medium, $\omega_p(z)$ is the beam waist at z position of the pump beam. For both positive and negative displacements of the sample from $z = 0$, the spot size of the pump beam increases almost symmetrically. The maximum average output power of 130 mW was obtained when the minimum pump beam spot was just on the rear surface of the Cr,Nd:YAG crystal. The average output power decreases when moving the Cr,Nd:YAG crystal forwards or backwards along the pump direction, as shown in Fig. 3. The decrease of the average output power was due to increase of the pump beam diameter on the Cr,Nd:YAG crystal; since the pump power intensity decreases with the increase of the pump beam diameter.
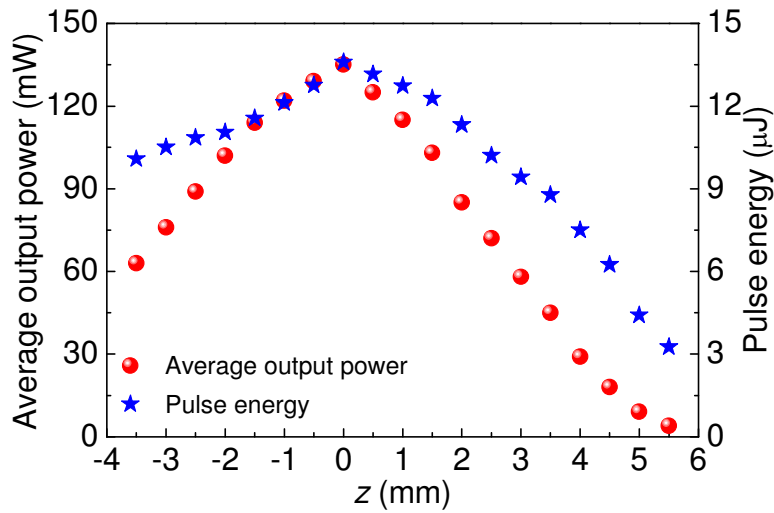

Fig. 3. The average output power and pulse energy of Cr,Nd:YAG self-Q-switched laser as a function of the position of the Cr,Nd:YAG sample along the pump beam [11].

In addition to the effect of the pump beam diameter on the transverse patterns as shown in Fig. 2, the temporal behaviors of the output pulse are also affected by the pump beam diameter on the Cr,Nd:YAG crystal. The temporal behavior of the output laser is a high repetition rate passively Q-switched pulse. The average pulse repetition rate is nearly proportional to the average output power. The highest repetition rate was achieved when the Cr,Nd:YAG crystal was close to the focus position of the pump beam. The repetition rate decreases with increase of the pump beam diameter incident on the Cr,Nd:YAG crystal under the same pump power. The pulse energy of the self-Q-switched laser was determined by the average output power and the pulse repetition rate. The pulse energy of the Cr,Nd:YAG self-

Q-switched laser depends on the beam waist of the pump beam and also is dependent on the transverse patterns of the output laser. The maximum output pulse energy at minimum pump beam diameter on the Cr,Nd:YAG crystal rear surface is estimated to be approximately 13.6 μJ. The pulse energy decreases with an increase of the pump beam diameter. The variation of pulse energy with position of the Cr,Nd:YAG sample along the pump beam propagation direction is also shown in Fig. 3. The pulse profiles varied with the focus position of the pump beam and exhibited pulse bifurcation or multi-pulse oscillation simultaneously, as shown in Fig. 4. The pulse width (FWHM) of each pulse in the pulse train was in the range from 3 ns to 19 ns. The pulse width (FWHM) and pulse profiles are strongly dependent on the pump beam diameter incident on the sample and the transverse patterns.
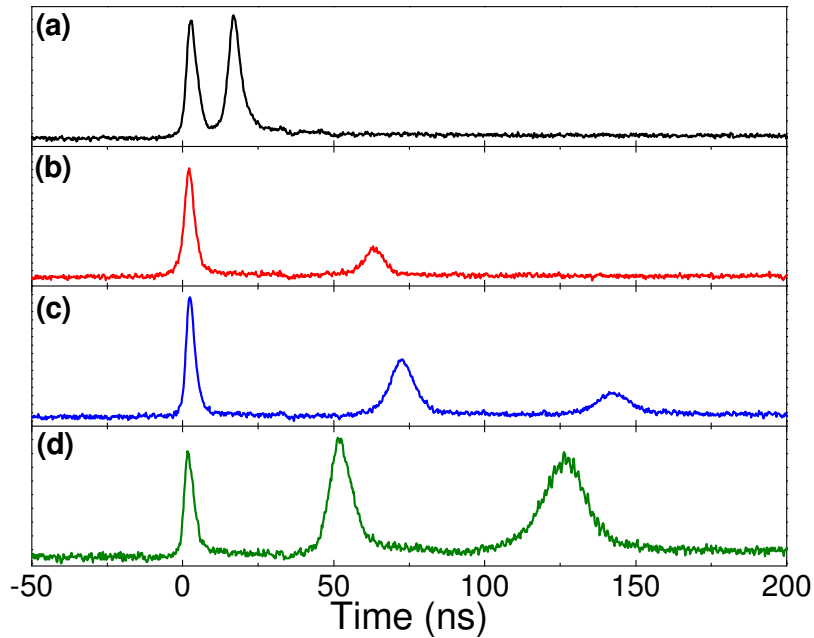

Fig. 4. The observed pulse profiles of Cr,Nd:YAG self-Q-switched laser with pump beam diameters when the Cr,Nd:YAG sample was positioned away from the focus point of the pump beam. (a) $z = -3$ mm; (b) $z = 0$ mm; (c) $z = 3.5$ mm; (d) $z = 5$ mm.

Two pulses oscillates simultaneously, one strong pulse followed by a weak pulse, when the pump beam was focused on the rear surface of the Cr,Nd:YAG crystal ($z = 0$), as shown in Fig. 4(b). The maximum peak power was estimated to be over 4.5 kW when the focus position was on the rear surface of the Cr,Nd:YAG crystal. Further increases in the pump beam diameter by moving the Cr,Nd:YAG sample closer to or further away from the focusing lens, the output pulse profiles as that at $z = 0$; with the discrepancy that the intensity ratio of the second pulse (or satellite pulse) to the main pulse varies with the pump power intensity. When the Cr,Nd:YAG sample was moved to $z \leq -3$ mm, the output pulse profile exhibits two-pulse bifurcation, as shown in Fig. 4(a). While the Cr,Nd:YAG sample was moved to $z \geq 3.5$ mm, the output pulse exhibits three-pulse oscillation, as shown in Fig. 4(c). Similar pulsation behavior in the three-pulse oscillation are maintained when the pump beam diameter is increased by moving the Cr,Nd:YAG sample further away from the focusing lens. The profiles and amplitudes of the pulses vary with an increase in the pump beam diameter. The relative intensities of the second pulse and third pulse increase compared to the first pulse as shown in Fig. 4(d). It is clear that there are more than two transverse modes oscillating simultaneously from the transverse beam pattern obtained at different positions as shown in Fig. 2 and the numerical reconstruction of the these patterns using different sets of Hermite-

Gaussian modes [11]. However, the two or three discrete laser pulses oscillating simultaneously suggest that strong mode coupling and competition exists between different transverse modes. The contribution from the transverse modes was synchronized by the mode coupling and competition in this passively Q-switched transverse-mode laser.
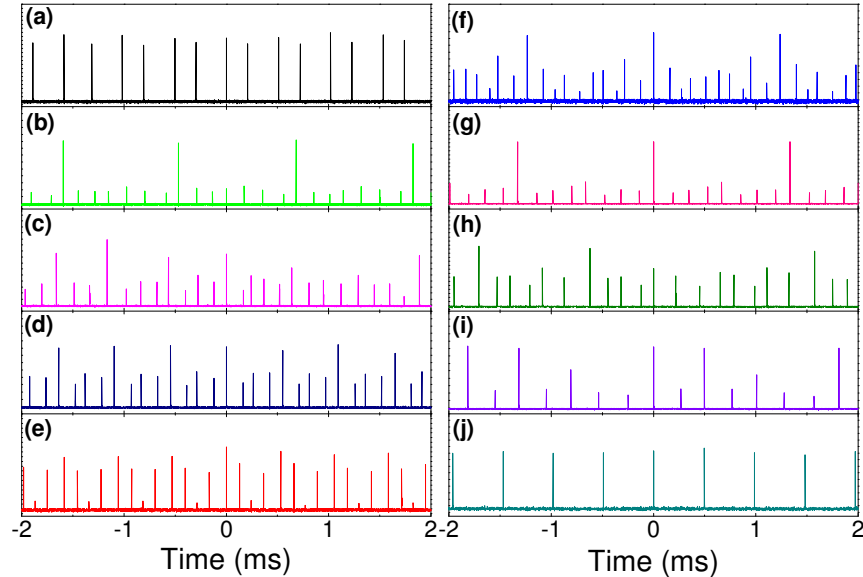

Fig. 5. The variation of pulse trains of Cr,Nd:YAG self-Q-switched laser when the Cr,Nd:YAG sample was set at different positions of the pump beam. (a) Period-2 pulsation oscillates when z = –3.5 mm; (b) period-7 pulsation oscillates when z = –3 mm; (c) period-4 pulsation oscillated when z = – 2 mm; (d) period-4 pulsation oscillates when z = – 0.5 mm; (e) period-4 pulsation oscillates when z = 0 mm; (f) period-10 pulsation oscillates when z = 1 mm; (g) period-8 pulsation oscillates when z = 2.5 mm; (h) period-6 pulsation oscillates when z = 3 mm; (i) period-7 pulsation oscillates when z = 4 mm; (i) period-1 pulsation oscillates when z = 5 mm.

The transverse modes not only have great effects on the pulse profiles of self-Q-switched Cr,Nd:YAG microchip lasers, but also have significant effects on the pulse trains. Figure 5 shows the variation in the observed pulse trains with periodical pulsation of the Cr,Nd:YAG self-Q-switched laser at different pump beam diameters when the Cr,Nd:YAG sample is set at different positions along the pump beam direction. The pulse trains exhibit period-5 pulsation at $z = 0$ as shown in Fig. 5(e). When the Cr,Nd:YAG crystal was at $z = 1$ mm, the pulse train is period-10 pulsation as shown in Fig. 5(f); further moving the Cr,Nd:YAG crystal away from the focus position, pulse trains were period-8 and period-6 pulsation at $z = 2.5$ mm and $z = 3$ mm, respectively. When the Cr,Nd:YAG sample is at $z = 4$ mm and 5 mm, the pulse trains are in period-7 and period-1 oscillation. The pulse train maintains a stable pulse height and repetition rate at $z = 5$ mm, such a state can be regarded as a good Q-switched laser. However, the average output power is low at $z = 5$ mm, as shown in Fig. 3 and three-pulse oscillation was observed as shown in Fig. 4(d). Further improvements in the stability of the Q-switched laser can be achieved using higher pump power under such large pump beam diameter at $z = 5$ mm. Owing to the different pump power spatial distribution along the thickness of the Cr,Nd:YAG sample, the pulse trains exhibit different periodical pulsation even with the symmetric pump beam diameter close to or away from the focus lens. When the Cr,Nd:YAG sample was moved towards to the focus lens, period-4 pulsation was observed when z is from –0.5 mm to –2.5 mm, as shown in Fig. 5(d) and Fig. 5(c). Further moving the Cr,Nd:YAG

crystal towards to the lens, period-7 and period-2 pulsation were observed at $z = -3$ mm and -3.5 mm, respectively, as shown in Fig. 5(b) and Fig. 5(a).

The pulse characteristics (pulse profiles and pulse trains) were not identical each other with the same pump beam diameter incident on the Cr,Nd:YAG crystal when the Cr,Nd:YAG sample was away from the focus position of the pump beam. The different transverse patterns and pulse characteristics at $z > 0$ and $z < 0$ show that the pump power distribution inside the thin gain medium has great effect on the laser pulse characteristics and the transverse pattern formation; the pump power distribution inside the Cr,Nd:YAG crystal cannot be neglected even in such thin gain medium. Besides the variation of the pulse characteristics with the pump beam diameter on the gain medium, the pulse trains also exhibited repetition rate jitter as shown in Fig. 5(a) – (i). The output pulsation characteristics of these microchip Cr,Nd:YAG lasers are attributed to the transverse mode coupling and competition mechanism due to the spatial hole burning and the nonlinear absorption of the Cr^{4+} saturable absorber.

For laser-diode pumped microchip lasers, the possible oscillating transverse modes are governed by the pump beam profile [9,16]. For small spatial pump widths, the overlap of higher-order transverse modes with the pump beam is low, leading to an increase of the threshold of higher-order modes for decreasing pump widths. However, for a large cross section of the pump beam, the thresholds of different transverse modes are nearly the same. The radius of TEM_{00} mode was estimated to be 52 μm according to [9], $w = (4\pi\lambda l/T_{oc})^{0.5}$, where λ is the laser wavelength, l is the cavity length and T_{oc} is the transmission of the output coupler. When the Cr,Nd:YAG crystal is set at $z = 0$, the pump beam waist is 150 μm, larger than the width of TEM_{00} mode. Other higher-order transverse modes can be excited under such large pump beam cross section. The pump power intensity decreases with further increase in the pump beam diameter incident on the Cr,Nd:YAG crystal. Higher-order transverse modes are suppressed at the edge of the pump region. Therefore, the oscillating modes decreases with increasing pump beam diameter. Owing to the different sets of the oscillating modes as shown in Fig. 2 under different pump beam diameters, the output pulses exhibit different pulse shapes such as three pulses oscillation simultaneously.

Owing to the thin Cr,Nd:YAG crystal and low pump power intensity used in the experiment, the laser was operated in single-longitudinal-mode oscillation. The instability and repetition rate jitter were attributed to multi-transverse-mode competition induced by the spatial-hole burning effect. The multi-pulse oscillation of the Cr,Nd:YAG self-Q-switched laser was attributed to the synchronization of different transverse modes with the nonlinear absorption effect of the Cr^{4+} saturable absorber.

4. Numerical simulations

To thoroughly understand the effect of the multi-transverse-mode of Cr,Nd:YAG self-Q-switched microchip laser on the laser pulse profile and periodical pulse trains, we modified the multimode laser rate equations by taking into account the mode-coupling dynamics that is due to the spatial hole-burning effect and the nonlinear absorption of the saturable absorber [22]. The modified rate equations for a passively Q-switched multimode laser of N transverse modes with the single-longitudinal-mode including the nonlinear absorption of the saturable absorber are introduced as follows [22–25]:

$$\frac{dn_u}{dt} = W - (\gamma_{20} + \gamma_{21})n_u - \sum_{i=1}^{N} C_i \left(n_u - n_l - \frac{n_i}{2} \right) \varphi_i c\sigma \quad (3)$$

$$\frac{dn_l}{dt} = -\gamma_{10}n_l + \gamma_{21}n_u + \sum_{i=1}^{N} C_i \left(n_u - n_l - \frac{n_i}{2} \right) \varphi_i c\sigma \quad (4)$$

$$\frac{dn_i}{dt} = C_i (n_u - n_l) \varphi_i c\sigma - n_i \left(\gamma_{21} + \sum_{i=1}^{N} C_i \varphi_i c\sigma \right) \quad (5)$$

$$\frac{d\varphi_i}{dt} = \frac{\varphi_i}{t_r}\left[\left(C_i 2\left(n_u - n_l - \frac{n_i}{2}\right)\sigma l - \ln\left(\frac{1}{R}\right) - L_i - 2\left(\sigma_g N_s + \sigma_e\left(N_0 - N_s\right)\right)l_s\right)\right] \quad (6)$$

$$\frac{dNs}{dt} = \left(N_0 - N_s\right)\gamma_s - \sigma_g c N_s \sum_{i=1}^{N}\varphi_i \quad (7)$$

with i = 1, …, N. In the Eq. (3) - 7), n_u and n_l are the population densities in the upper and lower laser levels; W is the pump rate, which is proportional to the pump power, and can be expressed as $W(r) = P_{in}\exp\left(-2r^2/w_p^2\right)\left(1 - \exp\left(-2\alpha l\right)\right)/\pi w_p^2 lh\nu_p$, where P_{in} is the incident pump power, w_p is the beam waist of the pump beam, l is the length of the gain medium, $h\nu_p$ is photon energy of the pump light, α is the absorption coefficient of gain medium; ϕ_i is the photon density of i-th mode; R is the reflectivity of the output coupler; L_i is the cavity loss for i-th mode; l_s is the length of the saturable absorber; c is the light of velocity in vacuum; $t_r = 2nl/c$, is the cavity round-trip time; σ is the stimulated emission cross section of gain medium; σ_g and σ_e are the ground-state and excited-state absorption cross section of the Cr^{4+}:YAG saturable absorber; N_{s0} and N_s are the total population density and population inversion density of Cr^{4+} satutrable absorber; C_i is the transverse-mode coupling coefficients respective to the fundamental transverse mode [26]. It should be noted that the mode coupling coefficient equal to 1 for two equal modes, and 0 for two modes that do not overlap at all, thus it may used as a measure to determine which modes are close in their transverse field distribution; γ_{20} and γ_{10} are the decay rates of the laser upper and lower energy levels to the ground state, respectively; γ_{21}, is the decay rate of the upper laser level to the lower laser level; γ_s is the recovery rate of the saturable absorber; n_i is the Fourier components of the population inversion density for the i-th mode, which can be described as follows:

$$n_i = \frac{2}{L_c}\int_0^{L_c} n(z,t)\cos\left(2k_i z\right)dz \quad (8)$$

where k_i is the wave number of transverse mode i and L_c is the length of the cavity filled with active medium.

Based on the parameters of our Cr,Nd:YAG laser (listed in Table 1), we numerically solved the rate equations to simulate the Q-switched pulse profiles and pulse trains by using the fourth-order Runge-Kutta method. A practical problem for numerically determining the passively Q-switched dynamics of the lasers is that some material parameters are not well known, e. g., two important parameters of Cr^{4+}:YAG crystal, ground-state and excited-state absorption cross-sections, σ_g and σ_e. The parameters of Cr^{4+}:YAG crystal is very difficult to determined because this material is very sensitive to the crystal growth atmosphere and annealing process, therefore, the ground-state and excited-state absorption cross section reported in the literature covers a wide range $\sigma_g = 3.6 \times 10^{-19} - 7 \times 10^{-18}$ cm^2 and $\sigma_e = 2.2 \times 10^{-19} - 2 \times 10^{-18}$ cm^2 [27–31]. As a comparison, in our numerical simulations, we have taken values of the parameters in the range of the reported ones. For quantitative comparison with the experimental results, we then used the values that give the closest results to the experimental results. Thus, for the numerical results reported here, two important parameters of Cr^{4+}:YAG crystal, $\sigma_g = 4.3 \times 10^{-18}$ cm^2 and $\sigma_e = 8.2 \times 10^{-19}$ cm^2 were used in the numerical simulations. Because broad area pump sources were used in these experiments, multi-transverse-modes were generated; the loss and spontaneous emission rate are assumed to be the same for all modes in the following numerical simulations for multi-transverse-mode oscillation. A typical numerical solution of the population inversion densities of three transverse modes, n_u-n_l-$n_l/2$, n_u-n_l -$n_2/2$, n_u-n_l -$n_3/2$, the population inversion density of the saturable absorber, N_s, and the photon density for three transverse modes oscillation, ϕ_1, ϕ_2, ϕ_3 are shown in Fig. 6(a). An incident pump power of 2.5 W, pump beam diameter of 380 μm and mode coupling coefficient $C_1 = 1$, $C_2 = 0.8$, $C_3 = 0.63$ were used in the numerical

simulations. The other laser parameters used in numerical calculations are listed in Table 1. The numerical solutions of three-pulse generation reproduced the experimental results shown in Fig. 4(c). The numerical simulation results of two pulses oscillation were shown in Fig. 6(b). An incident pump power of 2.5 W, the pump beam diameter of 150 μm and mode coupling coefficient $C_1 = 1$, $C_2 = 0.8$ were used in the numerical simulation, and the other parameters used in the simulations are listed in Table 1. The numerically calculated pulse profile was in good agreement with the observed pulse profile shown in Fig. 4(b). Other observed output pulse profiles shown in Fig. 4 can be easily obtained by adjusting the pump beam diameters and mode coupling coefficients, however, owing to the simplified rate equations, the pump power distribution along the pump beam direction was not considered in the rate equations, therefore, the differences observed between z > 0 and z < 0 cannot be simulated with the present simplified rate equations.
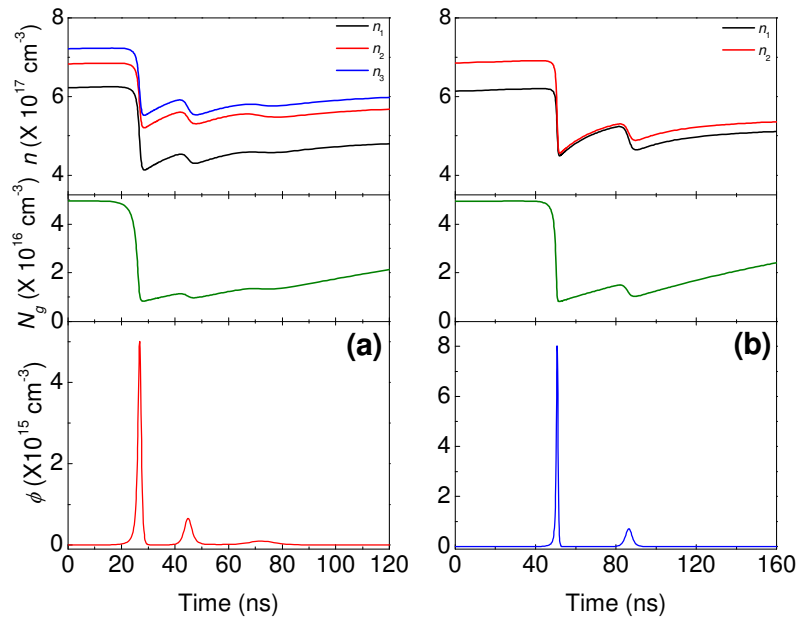

Fig. 6. Numerical simulations of the multi-pulse oscillation in self-Q-switched Cr,Nd:YAG multi-transverse-mode lasers. The evolutions of the inversion populations of gain medium, inversion populations of the Cr^{4+} saturable absorber, and the photon density of different pulses as a function of time, (a) three pulses oscillation under pump beam diameter of 380 μm; (b) two pulses generation under pump beam diameter of 150 μm.
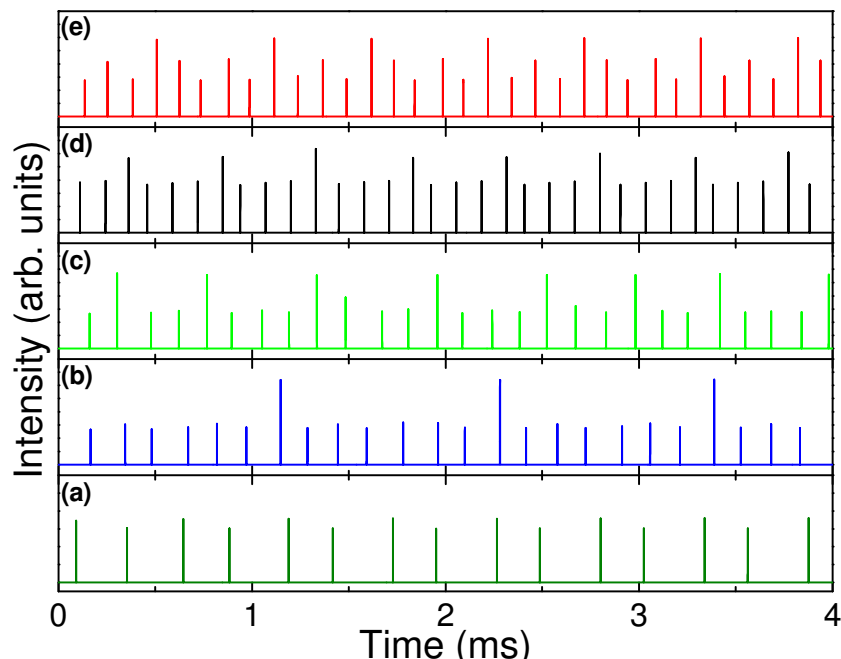
Fig. 7. Numerical simulations of the pulse trains under pump power of 2.5 W with different pump beam diameters (a) 380 μm, (b) 330 μm, (c) 250 μm, (d) 160 μm, (e) 150 μm, which are in good agreement with those observed in Fig. 4 (a) – (e).

The numerically calculated pulse trains under a pump power of 2.5 W with different pump beam diameters and different mode coupling coefficients ($C_1 = 1$, $C_2 = 0.8$, $C_3 = 0.63$ were used in the numerical simulations), as shown in Fig. 7 (a) – (e), not only reproduced observed output pulse trains under different multi-transverse-mode oscillations as shown in Fig. 5(a) – (e), but also clearly show that the pulse amplitudes and their pulse intervals vary periodically. These results show that the pump beam diameter plays an important role in the output pulse characteristics of self-Q-switched microchip lasers. A smaller pulse interval follows a larger pulse compared with the other pulse interval, suggesting that the pulse repetition rate's jitter is also an intrinsic property of the multi-transverse-mode laser system. The pulse amplitude fluctuations and the repetition rate jitter were reproduced in the numerical calculations irrespective of the initial conditions for the mode intensities and gains; the pulse amplitude fluctuation and repetition rate jitter generally exist at multi-transverse-mode oscillations. The time interval between the pulses is governed by the buildup time of the population inversion n to reach the threshold value, and also by the buildup time of the photon density, ϕ, which is very short compared to the buildup time of the population inversion under continuous-wave pumping, after n exceeds the threshold. Under the continuous-wave pumping, the fundamental mode of the laser will reach its threshold first while the higher-order transverse modes are suppressed. Therefore, the decrease of the population inversion of the fundamental mode, just after the oscillation, is more significant than that for the higher-order modes. After the pulse development for the fundamental mode, the population inversion for the fundamental mode was depleted dramatically compared to the higher-order modes. The recovery time of the population inversion to its threshold value is then shorter for the higher-order mode than for the fundamental mode, and the higher-order mode oscillation suppresses the fundamental mode. This kind of pulse train of multi-transverse-modes oscillates periodically under continuous-wave pumping and the nonlinear absorption of the saturable absorber. The delay time of each pulse is determined by the nonlinear absorption of the saturable absorber and the threshold for each mode. Similar pulsation behaviors of multi-transverse-mode oscillation

have been obtained generally for appropriate parameters under different pump beam diameters. The pulsation instability dynamics of multi-transverse-mode oscillation do change with the variation of the pump beam diameters, while the time interval between the pulses will be shortened with the decrease the pump beam diameters, as shown in Fig. 7(b) – (e). The time interval between each pulse for the total output pulse train is governed by the bleaching and recovery time of the population inversion of the Cr^{4+} saturable absorber.

Although there are some simplifications in the numerical calculations, the numerical simulations of the instability dynamics for the Cr,Nd:YAG self-Q-switched transverse-mode laser give us a clear image of the effects of the spatial hole burning of the gain medium and the nonlinear absorption of the saturable absorber on the dynamics of amplitude instability and repetition rate jitter. The good agreement between the experimental results and the numerical calculation of the instability and the repetition rate jitter for transverse-mode oscillation shows that the instability of the multi-transverse-mode oscillation is an intrinsic property of such lasers which is due to the spatial hole-burning effect of the gain medium and the nonlinear absorption of the saturable absorber.

Table 1. The parameters of Cr,Nd:YAG laser used in numerical simulations

Constant	Value	Reference
σ (cm^2)	2.35×10^{-19}	[32,33]
σ_g (cm^2)	4.3×10^{-18}	[29,31,34]
σ_e (cm^2)	8.2×10^{-19}	[29]
τ (μs)	210	[32,33]
τ_s (μs)	3.4	[29]
$h\nu_p$ (J)	2.46×10^{-19}	
$h\nu$ (J)	1.87×10^{-19}	
R (%)	5	
L_i	0.06	
N_{s0} (cm^{-3})	5×10^{16}	
l (mm)	1	
l_s (mm)	1	
λ_p (nm)	808	
λ (nm)	1064	
γ_{20}(s^{-1})	2762	[35]
γ_{21}(s^{-1})	2000	[35]
γ_{10}(s^{-1})	5×10^7	[35]

5. Conclusion

In conclusions, the effect of higher-order transverse modes on the laser characteristics (pulse profiles and pulse trains) was investigated experimentally and numerically in laser-diode pumped Cr,Nd:YAG self-Q-switched multi-transverse-mode microchip lasers. The pump beam diameter was found to have significant influence on the transverse modes, average output power, pulse repetition rate and pulse profile. The number of the transverse modes decreases with increase of the pump beam diameter incident on the Cr,Nd:YAG crystal under the same pump power. The multi-peak pulse oscillation was attributed to the broad pump beam diameter and the nonlinear absorption of the saturable absorber inside the gain medium. The peak power instability and the repetition rate jitter were also observed, which was due to the multi-transverse-mode competition. The numerical simulations of multi-pulse oscillation and periodical pulse trains under different pump beam diameters reproduced the observed multi-pulse oscillation and repetition rate instability and time jitter. The results show that the instability and time jitter of the multi-transverse-mode oscillation is an intrinsic property of

such laser which is due to spatial hole-burning of the gain medium and the nonlinear absorption of the saturable absorber.

Acknowledgements